

LETTER TO THE EDITOR

Trigonometric parallaxes of ten ultracool subdwarfs[★]

E. Schilbach¹, S. Röser¹, and R.-D. Scholz²

¹ Astronomisches Rechen-Institut, Zentrum für Astronomie der Universität Heidelberg, Mönchhofstraße 12-14, 69120 Heidelberg, Germany

e-mail: [elena,roeser]@ari.uni-heidelberg.de

² Astrophysikalisches Institut Potsdam, An der Sternwarte 16, 14482 Potsdam, Germany

e-mail: rdscholz@aip.de

Received 4 November 2008; accepted 25 November 2008

ABSTRACT

Aims. We measure absolute trigonometric parallaxes and proper motions with respect to many background galaxies for a sample of ten ultracool subdwarfs.

Methods. Observations were taken in the H -band with the OMEGA2000 camera at the 3.5m-telescope on Calar Alto, Spain during a time period of 3.5 years. For the first time, the reduction of the astrometric measurements was carried out directly with respect to background galaxies. We obtained absolute parallaxes with mean errors ranging between 1 and 3 mas.

Results. With six completely new parallaxes we more than doubled the number of benchmark ultracool ($>sdM7$) subdwarfs. Six stars in the M_{K_s} vs. $J - K_s$ diagram fit perfectly to model subdwarf sequences from M7 to L4 with $[M/H]$ between -1.0 and -1.5 , whereas 4 are consistent with a moderately low metallicity ($[M/H] = -0.5$) from M7 to T6. All but one of our objects have large tangential velocities between 200 and 320 km/s typical of the Galactic halo population.

Our results are in good agreement with recent independent measurements for three of our targets and confirm the previously measured parallax and absolute magnitude M_{K_s} of the nearest and coolest (T-type) subdwarf 2MASS 0937+29 with higher accuracy.

For all targets, we also obtained infrared J, H, K_s photometry at a level of a few milli-magnitudes relative to 2MASS standards.

Key words. Astrometry – Stars: distances – Stars: kinematics – Stars: low-mass, brown dwarfs – subdwarfs – solar neighbourhood

1. Introduction

Subdwarfs were originally defined by Kuiper (1939) as stars with spectral types A-K lying “not over 2-3 mag below the main sequence” in optical colour-magnitude diagrams. They are low-metallicity stars which have typically large space velocities. They are local representatives of the Galactic thick disk and halo populations and show up preferentially in high proper motion surveys. However, compared to thin disk stars with solar metallicities, subdwarfs are a rare species. In the well-investigated close solar neighbourhood ($d < 10$ pc) there are only 4 subdwarfs among the total of 348 objects with accurately measured trigonometric parallaxes (Henry et al. 2006).

The coolest subdwarfs with late-K and M spectral types have been described about ten years ago by Gizis (1997). He developed a corresponding spectroscopic classification scheme separating normal M dwarfs with solar metallicities ($[M/H] \approx 0.0$) from M subdwarfs (sdM) with metallicities $[M/H] \approx -1.2$ and extreme subdwarfs (esdM) with even lower metallicities ($[M/H] \approx -2.0$). The latest-type subdwarf classified by Gizis (1997) is the high proper motion star LHS 377 with a spectral type of sdM7.

The research of very low-mass stars and brown dwarfs has experienced an enormous progress for the last decade, mainly thanks to new deep optical and near-infrared (NIR) all-sky sur-

veys, which also enable and support new high proper motion searches. Many objects even cooler than M dwarfs have been discovered, the new spectral types L and T have been invented to describe them (see Kirkpatrick 2005 and references therein), and their current census has reached nearly 700 objects (Gelino et al. 2008). A question of particular interest is the formation of low-mass stars and brown dwarfs in the low-metallicity regime. Relicts of the early Galaxy and the first generations of star formation may be detectable among the faintest objects in the local Galactic halo population. Interestingly, the new sky surveys have also revealed a new population of ultracool subdwarfs (hereafter UCSDs), i.e. metal-deficient stars and brown dwarfs of spectral types later than sdM7 extending into the new L and possibly T spectral classes (Lépine et al. 2003b; 2003c; Scholz et al. 2004a; 2004b; Sivarani et al. 2004; Burgasser et al. 2002; 2003a; 2004; 2007; Burgasser & Kirkpatrick 2006; Lépine & Scholz 2008).

Trigonometric parallax measurements of these new UCSDs are essential to determine their absolute brightnesses, effective temperatures and space motions. The first (sub-)stellar UCSDs with accurate distance estimates will serve as benchmark sources for our understanding of this new population and for their detailed classification. A new classification scheme for UCSDs is still under debate (Gizis & Harvin 2006; Burgasser et al. 2007). Recently, Lépine et al. (2007) have revised the Gizis (1997) scheme for M subdwarfs and introduced a third class, the so-called ultrasubdwarfs (usdM), for the lowest metallicities. In contrast, Jao et al. (2008) have considered novel methods for assigning spectral types from K3 to M6 dwarfs, discrediting the previous subdwarf metallicity classes and suggesting in-

[★] Based on observations collected with Omega 2000 at the 3.5m telescope at the Centro Astronómico Hispano Alemán (CAHA) at Calar Alto, operated jointly by the Max-Planck Institut für Astronomie and the Instituto de Astrofísica de Andalucía (CSIC)

Table 1. Targets with previously known proper motions, JHK_s , photometry and spectral types

Name	J	H	K_s	SpType	Ref
	(2MASS)				
(1)	(2)	(3)	(4)	(5)	(6)
2MASS 0532+8246	15.179	14.904	14.918	sdL7	5;5,11
2MASS 0937+2931	14.648	14.703	15.267	d/sdT6	7;1,11
SSSPM 1013–1356	14.621	14.382	14.398	sdM9.5	3;3,11
SSSPM 1256–1408	14.011	13.618	13.444		12; -
SDSS 1256–0224	16.099	15.792	15.439	sdL4:	12;4,11
LSR 1425+7102	14.775	14.405	14.328	sdM8	12;8,11
SSSPM 1444–2019	12.546	12.142	11.933	d/sdM9	10;10,11
LSR 1610–0040	12.911	12.302	12.019	d/sdM7:†	12;2,11
2MASS 1626+3925	14.435	14.533	14.466	sdL4	6;6,11
LSR 2036+5059*	13.611	13.160	12.936	sdM7.5	12;9,11

References (col. 6, first index for proper motion, others for sp. type):

1 - Burgasser et al. (2002); 2 - Lépine et al. (2003c); 3 - Scholz et al. (2004a); 4 - Sivarani et al. (2004); 5 - Burgasser et al. (2003a); 6 - Burgasser (2004); 7 - Vrba et al. (2004); 8 - Lépine et al. (2003b); 9 - Lépine et al. (2003a); 10 - Scholz et al. (2004b); 11 - Burgasser et al. (2007); 12 - Scholz et al. (unpublished, preliminary proper motion solution based on available SSS and 2MASS data).

† - discovered by Lépine et al. (2003c) as the first possible L subdwarf. Cushing & Vacca (2006) described it as a very peculiar object (M6p/sdM), and Dahn et al. (2008) recently found it to be an astrometric binary of the Galactic halo population consisting of a mildly metal-poor M dwarf and a substellar companion.

* - Lépine et al. (2002) listed an erroneous position and proper motion for this object.

stead a more complex investigation of temperature, metallicity and gravity features. Such a three-dimensional scheme (temperature/clouds, metallicity, gravity) has also been proposed by Kirkpatrick (2005) for late-M, L and T dwarfs. However, the numbers of well-investigated subdwarfs are still too small (see Burgasser et al. 2007 for an overview) to fill the required grid of subtypes with benchmark sources.

2. Target selection

In 2004, when we initiated our subdwarf parallax programme, there were only nine UCSDs known, and all happened to be visible from a northern telescope site like Calar Alto. Among them, there were five M-type objects originally detected in optical high proper motion surveys by Lépine and co-workers (LSR 1425+7102, LSR 1610–0040, LSR 2036+5059) and Scholz and co-workers (SSSPM 1013–1356, SSSPM 1444–2019), three L- and T-type objects originally detected in the NIR Two Micron All Sky Survey (2MASS; Skrutskie et al. 2006) by Burgasser and co-workers (2MASS 0532+8246, 2MASS 0937+2931, 2MASS 1626+3925), and one object detected in the spectroscopic data base of the deep optical Sloan Digital Sky Survey (SDSS; York et al. 2000) by Sivarani et al. (2004). The 2MASS photometry, as well as spectral types from different sources are given in Table 1. We have included one more object (SSSPM 1256–1408), also detected in the high proper motion survey by Scholz et al. (unpublished) using the SuperCOSMOS Sky Surveys (SSS) data (Hambly et al. 2001), which is still lacking a spectral type. Its large optical-to-NIR ($R-J=+4.8$; R from SSS) and small NIR ($J-K_s=+0.57$) colour indices are however typical of late-M UCSDs.

When we started our observations, only one of our targets (2MASS 0937+2931) had a preliminary trigonometric parallax

measurement by Vrba et al. (2004). Meanwhile, there are three more parallaxes, all published in 2008, for 2MASS 0532+8246 (Burgasser et al. 2008), LSR 1425+7102 and LSR 1610–0040 (Dahn et al. 2008).

3. Observations and data reduction

The observations have been made with the OMEGA2000 camera at the 3.5m-telescope of the Centro Astronómico Hispano Alemán (CAHA) at Calar Alto, Spain. OMEGA2000 is a prime-focus, near-infrared, wide-field camera that uses a $2k \times 2k$ HAWAII-2 focal plane array with a sensitivity from the z to the K band. The optics of the camera consists of a cryogenic focal reducer providing a $15.4' \times 15.4'$ field of view with a resolution of $0.45''/\text{pixel}$. The astrometric observations were all obtained in the H -band. In all cases, at each epoch, we took 16 individual exposures of 60 s each (frames), with small offsets of a few arcseconds, thus totalling 16 minutes exposure time per object and night. The observations were taken between January 2005 and June 2008. The maximum epoch difference per target ranges from 3.1 to 3.4 years, with the number of useful epochs (nights) from 17 to 26. In addition, one observation (i.e., 16 individual frames) in the J and K_s bands has been taken for each target.

Object detection and centroiding was carried out by use of the SEXTRACTOR software (Bertin & Arnouts 1996). For the photometric reduction, standard stars are taken from 2MASS. On average, 100 stars per field with an accuracy better than 0.1 mag in 2MASS were used as a reference. In a given photometric band, each of 16 frames has been reduced to the 2MASS photometric system, separately. As a rule, a linear fit was sufficient for stars fainter than 9th mag. For each object in a field, the final J -, H -, and K_s -magnitudes were computed as averages of 16 values. The limiting magnitudes are slightly changing from field to field and they reach $J = 19$, $H = 18$, $K_s = 17.5$, at least.

For each target, the astrometric data reduction was performed in several steps. At first, an appropriate “reference” frame was chosen. Each frame was reduced to the “reference” frame using a classical 2nd-order polynomial fit. As reference points for the “frame-to-frame” reduction we use anonymous field stars with H magnitudes between 14 and 16.5; the number of reference stars varied between 75 for target 2MASS 0937+29 and 1250 for LSR 2036+5059. The “reference” frame was transformed to an intermediate equatorial reference system defined by 2MASS stars in a given sky area. Again, a 2nd-order plate fit was carried out. The number of reference stars from 2MASS varied between 85 and 1650, the latter in the field around LSR 2036+5059.

In this intermediate system, mean positions, proper motions and parallax were obtained via a rigorous single least-squares fit to the 5 unknowns, coupling the observational equations in R.A. and Dec. via the parallax factor. Although mathematically correct, the solution may suffer from a relatively short time baseline and a non-uniform distribution of observations. Thus correlations may influence the results for proper motions and parallax. In order to check the robustness of the solutions, two additional least-squares procedures were carried out. The first of these treated the equations in R.A. and Dec. separately, yielding two solutions for the parallax. In this check, correlations between R.A. and Dec. are prohibited. Evidently, the formal accuracy of the parallax is always better from R.A. than from Dec. Therefore, a weighted mean parallax was computed. The second

Table 2. Absolute parallaxes ($\pi(abs)$), absolute proper motions ($\mu_\alpha \cos \delta$, μ_δ), and infrared magnitudes (J, H, K_s) of ultracool Subdwarfs

Name	RA J2000.0 [h]	Dec J2000.0 [deg]	$\pi(abs)$ [mas]	Δ_π [mas]	$\mu_\alpha \cos \delta$ [mas/yr]	μ_δ [mas/yr]	J [mmag]	H [mmag]	K_s [mmag]	M_{K_s} [mag]	$V_{t(LSR)}$ [km/s]
2MASS 0532+82	5.548452	82.779208	42.28 ± 1.76	-3.36 ± 1.37	2039.46 ± 1.52	-1661.79 ± 1.64	15145 ± 8	14894 ± 5	14904 ± 15	13.03 ± 0.09	289 ± 12
2MASS 0937+29	9.626350	29.528189	163.39 ± 1.76	-3.39 ± 1.18	944.15 ± 1.24	-1319.78 ± 1.21	14622 ± 4	14677 ± 7	15407 ± 14	16.47 ± 0.03	53 ± 1
SSSPM 1013-13	10.218708	-13.939245	20.28 ± 1.96	-5.11 ± 1.24	69.44 ± 1.20	-1028.93 ± 1.33	14637 ± 7	14372 ± 5	14303 ± 7	10.84 ± 0.21	241 ± 23
SSSPM 1256-14	12.937228	-14.144533	18.76 ± 1.85	-0.38 ± 1.10	-741.11 ± 1.40	-1002.13 ± 1.38	14040 ± 4	13624 ± 5	13458 ± 5	9.82 ± 0.21	305 ± 31
SDSS 1256-02	12.943648	-2.414587	11.10 ± 2.88	-0.43 ± 1.11	-512.09 ± 1.90	-297.71 ± 1.79	16157 ± 13	16060 ± 8	16061 ± 22	11.29 ± 0.56	242 ± 66
LSR 1425+7102	14.418059	71.035998	12.19 ± 1.07	-0.73 ± 0.67	-602.38 ± 0.98	-177.71 ± 0.99	14828 ± 7	14412 ± 8	14245 ± 8	9.68 ± 0.19	240 ± 21
SSSPM 1444-20	14.738983	-20.323730	61.67 ± 2.12	-2.41 ± 1.48	-2906.15 ± 2.41	-1963.12 ± 2.71	12602 ± 6	12149 ± 4	11952 ± 4	10.90 ± 0.07	261 ± 9
LSR 1610-0040	16.174711	-0.681642	33.10 ± 1.32	-2.63 ± 0.95	-773.84 ± 0.91	-1231.58 ± 0.88	12872 ± 7	12304 ± 2	12004 ± 5	9.60 ± 0.09	205 ± 8
2MASS 1626+39	16.438927	39.422076	29.85 ± 1.08	-1.10 ± 0.48	-1374.14 ± 0.96	238.01 ± 0.87	14426 ± 5	14464 ± 9	14464 ± 10	11.84 ± 0.08	219 ± 8
LSR 2036+5059	20.606002	51.001279	21.60 ± 1.26	-1.00 ± 1.13	751.93 ± 1.10	1252.22 ± 1.31	13628 ± 9	13232 ± 5	12969 ± 20	9.64 ± 0.13	311 ± 19

checking approach is an iterative one. At first, only proper motions are computed. The solutions are taken to remove the proper motion effect from the observed image displacements. From the residuals, the parallax (and mean position again) is determined from the coupled equations. The iterations start with the removal of the parallax effect from the original observations, and determining proper motions from the latter. The procedure converged after 2 to 3 iterations. In this check, correlations between proper motions and parallax are prohibited. For all ten targets, the three solutions for the parallaxes differed by less than 40% of their combined mean error. Therefore, we consider our rigorous solution as reliable, stable and robust.

Because of the deep observations and the large field of $15.4' \times 15.4'$, an appropriate number of galaxies was found in each field, which were used to reduce the relative parallaxes and relative proper motions to absolute ones. Putting to zero the apparent parallaxes and proper motions of the galaxies yields the corrections converting relative parallaxes and relative proper motions to absolute ones for all other objects in the field. The images of all galaxies in the fields were visually inspected to select sufficiently compact, and well measured reference objects. The number of useful galaxies varied between 12 in the case of 2MASS 0532+82 to 105 in the case of SSSPM 1256-14.

4. Results and discussion

Table 2 compiles the astrometric and photometric results for the 10 targets. The first column contains the target's name. Columns 2 and 3 give the mean (barycentric) position (R.A. and Dec.) of the target for equinox and epoch J2000.0. Columns 4 and 5 present the absolute parallaxes $\pi(abs)$ and the applied corrections Δ_π converting the relative parallaxes to absolute ones as $\pi(abs) = \pi(rel) - \Delta_\pi$, while columns 6 and 7 give the derived absolute proper motions of the targets. Columns 8, 9, 10 summarize the results of our photometric measurements. Column 11 gives the absolute magnitude M_{K_s} , computed from the corresponding trigonometric parallax and K_s , whereas the last column lists the tangential velocities corrected for solar motion.

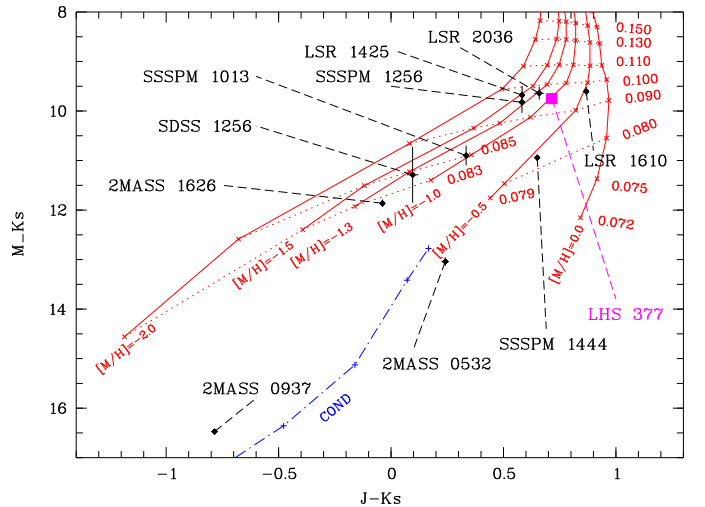


Fig. 1. Colour-absolute magnitude diagram M_{K_s} versus $J - K_s$ containing our 10 targets and the sdM7 LHS 377 (filled square), a late type subdwarf with an already measured parallax (Monet et al. 1992; Gizis 1997), plotted here for completeness. The error bars correspond to 1σ errors. The full (red) lines represent the absolute magnitudes and colours derived from the theoretical models by Baraffe et al. (1997) for 10 Gyr old objects with $[M/H]$ from -2.0 to -1.0 , and by Baraffe et al. (1998) for 5 Gyr old objects with $[M/H]$ from -0.5 to zero. The model data points were converted from the CTI photometric system to the 2MASS system using the Carpenter (2001) transformations. Dotted lines are the lines of equal mass. The pluses connected by the dashed-dotted line show COND model points for 5 Gyr old objects with less than 0.075 solar masses (Baraffe et al. 2003).

Four of our targets have trigonometric parallaxes already published. These are 2MASS 0532+82 with $\pi = 37.5 \pm 1.7$ mas ($M_{K_s} = 12.79 \pm 0.18$ mag) by Burgasser et al. (2008), 2MASS 0937+29 with $\pi = 162.84 \pm 3.88$ mas ($M_{K_s} = 16.46 \pm 0.14$ mag) by Vrba et al. (2004), LSR 1425+7102 and LSR 1610-0040

with, respectively, $\pi = 13.37 \pm 0.51$ mas ($M_{K_s} = 9.97 \pm 0.13$ mag) and $\pi = 31.02 \pm 0.26$ mas ($M_{K_s} = 9.48 \pm 0.04$ mag) both by Dahn et al. (2008). All these parallaxes are based on observations with the 1.55 m Strand Astrometric Reflector at the USNO Flagstaff Station. The number of reference stars used varied between 6 and 16. Photometric data were taken mainly from the 2MASS Catalog. In spite of the different observation and reduction techniques, the published parallaxes coincide reasonably well with our results, i.e. the differences between two corresponding values are smaller than 2 times their mean errors. The parallax solutions from the observations with the 1.55 m Strand Astrometric Reflector take advantage of a better scale ($\approx 0.35''/\text{pixel}$ versus $\approx 0.45''/\text{pixel}$), and, for LSR 1425+7102 and LSR 1610-0040, of considerably larger ranges of epochs and numbers of nights. On the other hand, we benefit from a better SNR for the fainter targets, especially for photometry where the 2MASS Catalog is almost at its limit. Moreover, a relatively wide and deep field allows to use a large number of reference stars and, for the first time, to derive parallaxes directly with respect to galaxies and, consequently, to reduce a possible systematic bias in the parallax determination.

From the tangential velocities we infer that all objects except 2MASS 0937+29 exhibit halo kinematics. Postponing the discussion of the latter, we find that the remaining targets split into two groups in the CMD of Fig. 1. The first group is related to metallicity $[M/H] = -0.5$ in the Baraffe et al. (1997) isochrones for metal-poor low-mass stars, and is occupied by the objects LSR 1610-0040, SSSPM 1444-20 and 2MASS 0532+82. Ordered by luminosity they were classified as d/sdM7, d/sdM9 and sdL7 in Burgasser et al. (2007), respectively. For the first two objects, this is consistent with the Gizis (1997) classification scheme that rates dwarfs “d” with $[M/H] \approx 0$, and subdwarfs “sd” with $[M/H] \approx -1.2$. Note that 2MASS 0532+82, extensively discussed by Burgasser et al. (2008) fits perfectly to the locus of $[M/H] = -0.5$, and therefore is not an real subdwarf according to the Gizis (1997) classification. Its moderately low metallicity has also been suggested by Scholz et al. (2004b) based on comparison with model colours ($I-J$ and $J-K$). Therefore, we think these three objects can be used as benchmarks for the type “d/sd” with $[M/H] = -0.5$ from M7 to L7.

Of the remaining 6 objects only one has a previously determined trigonometric parallax, LSR 1425+7102, measured by Dahn et al. (2008), and classified as sdM8 by Burgasser et al. (2007). The sdM7 LHS 377, which was not on our target list, is a close neighbour to LSR 1425+7102 in the CMD. All our 6 objects populate the area between $[M/H] = -1.0$ and $[M/H] = -1.5$ in the Baraffe et al. (1997) isochrones. All are classified as “sd” by Burgasser et al. (2007) except our newly detected object SSSPM 1256-14, which we would classify as sdM8 based on its position in the CMD. The coolest object, the sdL4 2MASS 1626+39 has $M/M_\odot = 0.083$ and $T_{\text{eff}} = 2300$ K when compared with the Baraffe et al. (1997) isochrones for $[M/H] = -1.0$. Our faintest (by apparent magnitude) target SDSS 1256-02 had the K_s magnitude in 2MASS given with a problem flag. Its 2MASS colour of $J-K_s = 0.66$ changes into 0.09 according to our photometry, and hence its metallicity in the Baraffe et al. (1997) models changes from -0.5 to -1.3 .

Our 6 targets as well as LHS 377 serve as benchmarks for the subdwarf population between M7 (LHS 377) and L4 (2MASS 1626+39) in the metallicity range between $[M/H] = -1.0$ and -1.5 . Baraffe et al. (2003) recently published new evolutionary models for the coolest brown dwarfs (T dwarfs), which they refer to as the COND models. In these models, dust opacity in the

radiative transfer equation is neglected. The COND isochrone is shown in Fig. 1 only for objects with $M/M_\odot < 0.075$. For masses up to $M/M_\odot = 0.08$ it formally coincides with the $[M/H] = -0.5$ isochrone. So, our targets from the $[M/H] = -0.5$ group have loci close to the COND isochrone, but the targets from the $[M/H] = -1.3$ class lie significantly above this isochrone.

2MASS 0937+29 may be the faintest object along the extrapolated $[M/H] = -0.5$ isochrone in Fig. 1. It was also characterised as slightly metal-poor ($-0.4 < [M/H] < -0.1$) by Burgasser et al. (2003b; 2006) using spectral model comparisons. Compared to the 2MASS colour, our new photometry lead to a bluer $J - K_s$, which is again supporting a sub-solar metallicity if we compare its location in Fig. 1 with the COND model points. Its relatively low tangential velocity $V_{t(LSR)}$ of about 50 km/s does not, however, reject a higher spatial velocity of 2MASS 0937+29 with respect to the local standard of rest (LSR). The presently unknown V_{rad} of 2MASS 0937+29, contributes to its space velocity components as $(U, V, W)_{LSR} = (38 - 0.64V_{\text{rad}}, -30 - 0.21V_{\text{rad}}, +0.74V_{\text{rad}})$. Therefore, as long as the radial velocity of 2MASS 0937+29 is unknown, one cannot exclude the possibility that 2MASS 0937+29 is a member of the thick disk or even of the halo population.

In summary, we have measured infrared trigonometric parallaxes of ten ultracool subdwarf, for 6 of which for the first time. The absolute parallaxes have referred to galaxies directly, also for the first time. Compared to theoretical models, 4 stars have moderately low metallicity, $[M/H] \approx -0.5$, whereas 6 are consistent with $[M/H]$ between -1.0 and -1.5 . Nine out of ten definitely show halo kinematics from their tangential velocities, while 2MASS 0937+29 needs a large radial velocity to be kinematically excluded as a member of the disk.

References

- Baraffe, I., Chabrier, G., Allard, F., & Hauschildt, P. H. 1997, A&A, 327, 1054
 Baraffe, I., Chabrier, G., Allard, F., & Hauschildt, P. H. 1998, A&A, 337, 403
 Baraffe, I., Chabrier, G., Barman, T. S., Allard, F., & Hauschildt, P. H. 2003, A&A, 402, 701
 Bertin, E. & Arnouts, S., 1996, A&AS, 117, 393
 Burgasser, A. J. 2004, ApJ, 614, L73
 Burgasser, A. J., Kirkpatrick, J. D., Brown, M. E., et al. 2002, ApJ, 564, 421
 Burgasser, A. J., Kirkpatrick, J. D., Burrows, A., et al. 2003a, ApJ, 592, 1186
 Burgasser, A. J., Kirkpatrick, J. D., Liebert, J., & Burrows, A. 2003b, ApJ, 594, 510
 Burgasser, A. J., & Kirkpatrick, J. D. 2006, ApJ, 645, 1485
 Burgasser, A. J., Kirkpatrick, J. D., & Burrows, A. 2006, ApJ, 639, 1095
 Burgasser, A. J., Cruz, K. L., & Kirkpatrick, J. D. 2007, ApJ, 657, 494
 Burgasser, A. J., Vrba, F. J., Lépine, S., et al. 2008, ApJ, 672, 1159
 Carpenter, J. M. 2001, AJ, 121, 2851
 Cushing, M. C., & Vacca, W. D. 2006, AJ, 131, 1797
 Dahn, C. C., et al. 2008, ApJ, 686, 548
 Gelino, C. R., Kirkpatrick, J. D., & Burgasser, A. J. 2008, online database for 670 L and T dwarfs at DwarfArchives.org (status: 30 September 2008)
 Gizis, J. E. 1997, AJ, 113, 806
 Gizis, J. E., & Harvin, J. 2006, AJ, 132, 2372
 Hambly, N. C., MacGillivray, H. T., Read M. A., et al. 2001, MNRAS, 326, 1279
 Henry, T. J., Jao, W.-C., Subasavage, et al. 2006, AJ, 132, 2360
 Jao, W.-C., Henry, T. J., Beaulieu, T. D., & Subasavage, J. P. 2008, AJ, 136, 840
 Kirkpatrick, J. D. 2005, ARA&A, 43, 195
 Kuiper, G. P. 1939, ApJ, 89, 548
 Lépine, S., Shara, M. M., & Rich, R. M. 2002, AJ, 124, 1190
 Lépine, S., Rich, R. M., & Shara, M. M. 2003a, AJ, 125, 1598
 Lépine, S., Shara, M. M., & Rich, R. M. 2003b, ApJ, 585, L69
 Lépine, S., Rich, R. M., & Shara, M. M. 2003c, ApJ, 591, L49
 Lépine, S., Rich, R. M., & Shara, M. M. 2007, ApJ, 669, 1235
 Lépine, S., & Scholz, R.-D. 2008, ApJ, 681, L33
 Monet, D. G., Dahn, C. C., Vrba, F. J. et al. 1992, AJ, 103, 638
 Scholz, R.-D., Lehmann, I., Matute, I., & Zinnecker, H. 2004a, A&A, 425, 519

- Scholz, R.-D., Lodieu, N., & McCaughrean, M. J. 2004b, A&A, 428, L25
Sivarani, T., Kembhavi, A. K., & Gupchup, J. 2004, submitted to ApJ Letters
Skrutskie, M. F., Cutri, R. M., Stiening, R., et al. 2006, AJ, 131, 1163
Vrba, F. J., Henden, A. A., Luginbuhl, C. B., et al. 2004, AJ, 127, 2948
York, D. G., Adelman, J., Anderson, J. E., et al. 2000, AJ, 120, 1579